Excited State Charge Transfer Enabling MoS_2/Phthalocyanine Photodetectors with Extended Spectral Sensitivity

Niklas Mutz,[†] Soohyung Park,[‡,§] Thorsten Schultz,[‡,∥] Sergey Sadofev,[‡] Simon Dalgleish,[†] Louisa Reissig,[¶] Norbert Koch,[‡,∥] Emil J. W. List-Kratochvil,[†] and Sylke Blumstengel[*,†]

[†]*Institut für Physik, Institut für Chemie & IRIS Adlershof, Humboldt-Universität zu Berlin, Brook-Taylor-Str. 6, 12489 Berlin, Germany*

[‡]*Institut für Physik & IRIS Adlershof, Humboldt-Universität zu Berlin, Brook-Taylor-Str. 6, 12489 Berlin, Germany*

[¶]*Institut für Experimentelle Physik, Freie Universität Berlin, Arnimallee 14, 14195 Berlin, Germany*

[§]*Advanced Analysis Center, Korea Institute of Science and Technology (KIST), Seoul 02792, Republic of Korea*

[∥]*Helmholtz-Zentrum Berlin für Materialien und Energie GmbH, Albert-Einstein-Str. 15, 12489 Berlin, Germany*

E-mail: sylke.blumstengel@physik.hu-berlin.de

Abstract

Monolayer (ML) transition metal dichalcogenides (TMDCs) are an attracting new class of two-dimensional direct band gap semiconducting materials for optoelectronic device applications. The combination of TMDCs with organic semiconductors holds the promise to further improve device properties with added functionality. Here we demonstrate that excited state charge transfer from a thin organic absorber layer, i.e. metal-free phthalocyanine (H_2Pc), enhances the photoresponse of ML MoS_2 dramatically and at the same time also significantly extends it to spectral regions where the TMDC is transparent. The fundamental processes enabling this boost in photodetector performance are unraveled by a combination of photoemission (PES), photoluminescence (PL) and photocurrent action spectroscopy. Direct and inverse PES reveal a type II energy level alignment at the MoS_2/H_2Pc interface with a large energy offset of 1 eV, which is sufficient to drive the excited state charge transfer. Time-resolved PL measurements evidence highly efficient dissociation of excitons generated in H_2Pc when they are in contact with MoS_2. Exciton dissociation results in the formation of a charge-separated state at the hybrid interface with an energy gap of ca. 1.2 eV, in accordance with PES. This state then dissociates into free carriers and markedly contributes to the current in the photodetector, as demonstrated by photocurrent action spectroscopy. This reveals that the photoconductivity within the MoS_2 ML is generated by light directly absorbed in the TMDC and, notably, with comparable efficiency by the absorption of H_2Pc. The present demonstration of highly efficient carrier generation in TMDC/organic hybrid structures paves the way for future nanoscale photodetectors with very wide spectral sensitivity.

Introduction

Group-VI TMDCs have emerged in recent years as promising candidates for semitransparent, ultrathin and flexible (opto)electronic devices. In the ML regime these materials feature a direct band gap and a high exciton binding energy.[1,2] As a result, TMDCs possess very large light-matter interaction cross sections. Furthermore, being covalent crystals, the charge carrier mobilities can reach values up to 100 $cm^2/(Vs)$.[3,4] Further enhancement of the properties and added functionality are expected upon combination of TMDC MLs with conjugated organic molecules. For example, the absorption of normal incidence light at the excitonic resonances of TMDC MLs is less than 10 % despite their large light-matter interaction cross section, since the active layer consists just of three atomic layers. Functionalization of such MLs with an organic absorber layer can help to enhance the photon harvesting and detection capabilities of TMDC based devices while maintaining the monolayer nature of the TMDC. A prerequisite is that the excitation energy deposited in the organic absorber is transferred to the TMDC layer. Two processes are possible, namely Förster-type resonant energy transfer (FRET) or excited state charge transfer. The occurrence of these processes at a few TMDC/organic interfaces has already been shown.[5–9] In the FRET-process, electron-hole pairs, e.g. excitons, excited in the organic layer are converted to excitons in the TMDC layer where they can contribute to the photoconductivity. FRET requires spectral overlap between the TMDC absorption and the molecule's PL. Consequently, also the absorption of the molecular layer will overlap with the TMDC absorption. In such a configuration, an increase of the overall absorption cross section of the structure can be achieved.[6] The charge transfer route requires a staggered (type II) energy level alignment at the TMDC/organic interface with sufficiently large energy offsets between the frontier molecular orbital levels and the valence and conduction band edges of the two-dimensional semiconductor to drive efficient exciton dissociation. Overlap of the optical spectra is not required. Therefore, besides an increase of the overall absorption cross section also an extension of spectral sensitivity range for photodetection to regions, where the TMDC ML does not absorb, can be achieved

by proper choice of the molecules.

In the present work we follow the charge-transfer approach and combine a metal-free phthalocyanine (H_2Pc) with a MoS_2 ML. Phthalocyanine (Pc) and its metal derivatives (metal-Pc), commonly used in organic photovoltaic devices and distinguished by their excellent chemical stability, have recently been discussed to undergo charge transfer interactions with various TMDCs (MoS_2, $MoSe_2$, WSe_2).[10–17] Their foreseeable potential for enhancing the photoresponse in TMDC-based phototransistors merits an in-depth investigation of the charge transfer processes and the mechanisms of the photocurrent generation at TMDC/phthalocyanine interfaces. In this study, we determine the electronic structure of the H_2Pc/MoS_2 hybrid interface with direct and inverse PES and find that ground state charge transfer can be ruled out, while excited state charge transfer is possible due to a type II energy level alignment at the H_2Pc/MoS_2 hybrid interface with energy offsets larger than the exciton binding energies in both materials. Indeed, continuous-wave and time-resolved PL spectroscopy reveal efficient exciton dissociation at the hybrid interface, resulting in the generation of a charge-separated state with the hole residing in H_2Pc and the electron in MoS_2. The subsequent generation of free charge carriers is evidenced by photocurrent action spectroscopy of reference single-component and hybrid H_2Pc/MoS_2 photodetectors. The spectra demonstrate that in the hybrid device the photoresponse of the MoS_2 ML is strongly enhanced and furthermore extended into spectral regions where the TMDC is transparent.

Experiment

Photoemission spectroscopy: Ultraviolet (UPS) and X-ray (XPS) photoemission spectroscopy were performed using a Phoibos-100 spectrometer using a He discharge lamp (21.2 eV) and a Mg X-ray anode (1253.6 eV), respectively, as excitation sources. For the measurement of the secondary electron cutoff (SECO) the sample was biased at -10 V to clear the analyzer work function. The inverse photoemission (IPES) measurements were conducted

in the isochromat mode, using a low-energy electron gun with a BaO cathode and a band pass filter of 9.5 eV (SrF_2 + NaCl). Prior to the measurements, the MoS_2 MLs on SiO_2 (2D Semiconductors) were annealed at 300 °C over night in UHV. Subsequently, the H_2Pc was evaporated from resistively heated quartz crucibles and the measurements performed *in situ* for different molecular coverages. UPS and IPES spectra of the pristine MoS_2 surface were recorded at an emission and incident polar angle of 36° and 70°, respectively, to probe the K-point,[18] while for the MoS_2/H_2Pc interfaces the spectra were recorded only at normal incidence probing the Γ-point.

Continuous wave (cw) and time-resolved PL spectroscopy: The experiments were performed at a μ-PL set-up using laser diodes (Picoquant) emitting at 2.21 eV and 1.95 eV as excitation sources. The average intensity was 14 kW/cm^2 for cw and 24 kW/cm^2 for time-resolved measurements (80 MHz pulse repetition rate). PL transients were recorded employing time-correlated single photon counting. MoS_2 MLs were grown by pulsed thermal deposition on SiO_2 substrates.[19] Reference MoS_2 and hybrid MoS_2/H_2Pc were prepared by vacuum deposition of a 1 nm-thick H_2Pc film through a shadow mask on a MoS_2 ML to define covered and uncovered areas. For the measurements, the samples were transferred without contact to ambient atmosphere to a measuring chamber evacuated to $5{\cdot}10^{-5}$ mbar to prevent photooxidation of H_2Pc under intense laser irradiation as well as to slow down the dewetting of the layer.

Photocurrent action spectroscopy: Hybrid MoS_2/H_2Pc as well as reference H_2Pc-only and MoS_2-only photodetectors were prepared on SiO_2 substrates coated with a benzocyclobutene (BCB)-based polymer layer. The BCB layer was prepared from a solution of cyclotene 3022-35 (Dow chemicals, diluted with 2 parts mesitylene) by spin coating onto a SiO_2 substrate. Cross-linking of the BCB molecules is achieved by annealing at 270 °C for ten minutes in a nitrogen-filled glovebox. Subsequently, thin gold electrodes with a distance of 30 µm were deposited via evaporation through shadow masks. Continuous MoS_2 MLs of 1 x 1 cm^2 size (2D Semiconductors) were transferred via a polystyrene-based wet transfer

process onto the BCB layer with the predeposited contacts following the recipe described in literature.[20] The hybrid photodetector was finished by evaporation of a nominally 3-nm-thick H_2Pc film onto MoS_2. In the reference MoS_2-only photodetector, the H_2Pc layer was omitted. The reference H_2Pc-only photodetector was prepared by deposition of a nominally 3-nm-thick layer on BCB. Photocurrent action spectra were recorded illuminating the devices by a tungsten/halogen light source (Spectral Products ASBN-W 150F-L) attached to a dual grating monochromator (Digikröm CM110), and modulated by a chopper. The photocurrent signals were pre-amplified using a low noise transimpedance amplifier (Femto, DLPCA 200) and extracted using a lock-in amplifier (Perkin Elmer 7265 DSP). The photoresponse was calculated by dividing the photocurrent signal by the wavelength-dependent light power.

Results and discussion

A prerequisite for the understanding of charge transfer processes at interfaces between MoS_2 and H_2Pc is a precise knowledge of the energy positions of the occupied and unoccupied levels of the two materials when brought into contact. Therefore we discuss the results of the PES first. Since the bandgap of TMDCs depends on the dielectric environment,[21] the choice of the substrate will influence the energy level alignment of the hybrid interface as well. Here we use SiO_2, as it is typically used as gate dielectric in hybrid phototransistors.[13,15] Figure 1a and b show the SECO as well as UPS and IPES for incremental depositions of H_2Pc on MoS_2. In order to properly determine the energies of the valence band maximum (VBM) and the conduction band minimum (CBM) of the pristine MoS_2 surface, UPS and IPES recorded at the K-point of the Brillouin zone are depicted.[18,22] Since band dispersion in H_2Pc is negligible, the measurements of the MoS_2/H_2Pc interfaces were performed at normal incidence only, probing the Γ-point. In addition, no valence band distortions of MoS_2 are expected upon deposition of the molecules according to an earlier work about the interface between a molecular dopant and a MoS_2 ML, suggesting that any momentum

line cut will provide the same information in terms of energy and feature of the density of states.[23] The SECO positions and all binding energy onsets were determined from the intersection of two straight lines defined by the baseline and the linear region of the spectra slope. The work function ϕ of the bare MoS_2 ML is found to be 3.9 eV. Upon deposition of 0.5 nm of H_2Pc, ϕ increases only slightly by 80 meV and then stays constant upon further increase of the organic layer thickness (Fig. 1a). The level onsets of the valence features are found at binding energies of 1.8 eV for the MoS_2 VBM and 0.9 eV for the H_2Pc highest occupied molecular orbital (HOMO) below the Fermi level (Fig. 1b), yielding ionization energies of 5.7 eV and 4.9 eV for MoS_2 and H_2Pc, respectively, in agreement with previous reports.[24,25] No energy shift of the valence features is observed with increasing organic layer deposition. The positions of the unoccupied levels are derived from IPES. Here, the level onsets are found at 0.3 eV for the MoS_2 CBM and at 1.3 eV for the H_2Pc lowest unoccupied molecular orbital (LUMO) above the Fermi level (Fig. 1b). The core levels are investigated by XPS. No energy shift of the core level features is observed as a function of the organic layer thickness as exemplary shown for the Mo $3p_{3/2}$ and the N 1s spectra in Fig. 1c (see supporting information for the Mo 3d and S 2p spectra). The insignificant change in the work function and the absence of any shift in the valence and core level features are clear indications that ground state charge redistribution at the MoS_2/H_2Pc interface is negligible. The occurrence of ground state charge transfer has recently been controversially discussed at the zinc phthalocyanine/MoS_2 interface.[15,17] At the present MoS_2/H_2Pc interface it can be ruled out. On the other hand, the prerequisite for excited state charge transfer is fulfilled as immediately apparent from the energy level diagram depicted in Fig. 2. The MoS_2/H_2Pc interface forms a type II heterostructure with energy offsets between the occupied and the unoccupied levels amounting to 900 meV and 1 eV, respectively. Therefore, electron transfer from the H_2Pc LUMO to the MoS_2 conduction band as well as hole transfer from the MoS_2 valence band to the H_2Pc HOMO is energetically favorable.

To investigate excited state charge transfer at the MoS_2/H_2Pc interface, continuous-wave

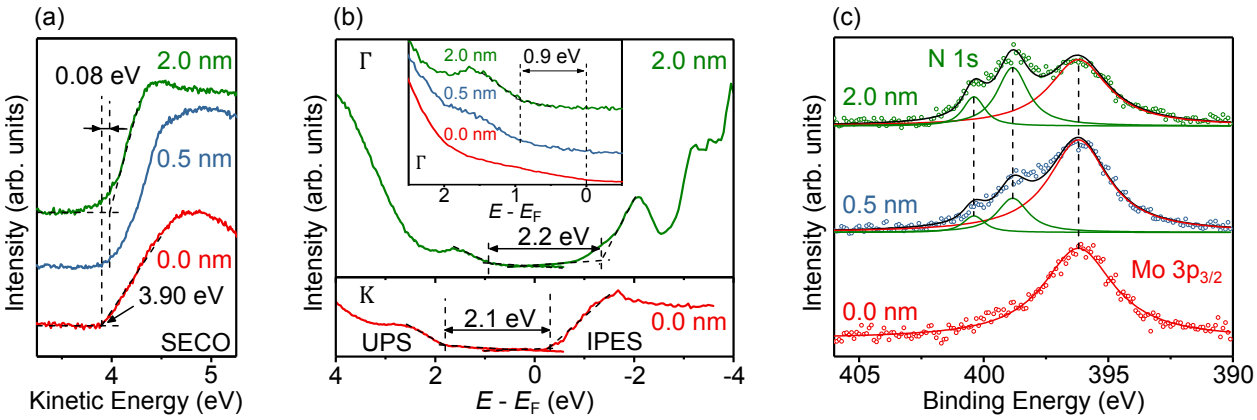

Figure 1: Evolution of the work function ϕ (a) and of the occupied and unoccupied levels (b) at MoS_2/H_2Pc interfaces with increasing H_2Pc coverage. The MoS_2 spectra were recorded at the K-point to obtain the positions of the VBM and the CBM, while the H_2Pc spectra were measured at the Γ-point since band dispersion is negligible in the molecular layer. The HOMO and LUMO as well as VBM and CBM positions are indicated by dashed lines. The inset shows a magnification of the VB region at the Γ-point. To obtain a more accurate CBM onset, the IPES spectra were deconvoluted.[18] The raw data are reported in the Supporting Information. The error of the deduced binding energies is ±50 meV. (c) Mo $3p_{3/2}$ and N 1s core level spectra for incremental deposition of H_2Pc.

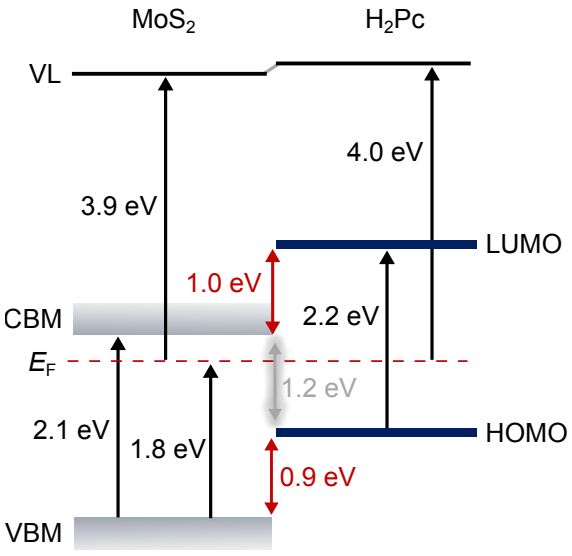

Figure 2: Energy level diagram of the MoS_2/H_2Pc interface derived from UPS and IPES.

and time-resolved PL measurements were performed. Prior to the discussion of the hybrid interface, the optical properties of the individual constituents are presented (see Fig. 3a). The absorption spectrum of the H_2Pc layer on SiO_2 is comprised of the Soret band > 3 eV and the Q-band with two main features at 1.94 eV and 1.78 eV and a shoulder at 2.14 eV.[26] The spectrum is similar to that reported previously for the H_2Pc α-phase.[27,28] Compared to the spectrum in solution, the Q-band absorption is blue-shifted and broadened due to aggregation.[27,28] The high energy shoulder has been previously assigned to a transition with charge transfer character in metal-Pc films.[29] The weak PL signal at 1.4 eV originates from the Q-band. The MoS_2 absorption spectrum features the A, B and C excitonic transitions at 1.91 eV, 2.05 eV and 2.90 eV, respectively. The comparison of the absorption spectra shows that the optical gap of H_2Pc is smaller than that of MoS_2. This is in contrast to the single particle gap derived from UPS and IPES, which is slightly larger for H_2Pc (see Fig. 2) as a result of the larger exciton binding energy in the organic material. The comparison of the optical gap derived from absorption measurements and the single particle gap yields exciton binding energies of ca. 420 meV for H_2Pc and ca. 220 meV for MoS_2 in the present configuration. The PL originating from the A excitonic transition of the TMDC overlaps well with the Q-band absorption of the molecular layer (see Fig. 3a). Therefore, FRET from MoS_2 to H_2Pc is possible while in the other direction it is prohibited.

The PL and absorption spectra of the MoS_2/H_2Pc hybrid structure are shown in Fig. 3b. The hybrid structure was obtained by covering half of the area of the MoS_2 reference sample with H_2Pc. The PL shows two distinct peaks stemming from H_2Pc (1.42 eV) and MoS_2 (1.89 eV). The PL peak of H_2Pc on MoS_2 is shifted to lower energies by ca. 30 meV with respect to the spectrum recorded on SiO_2 while the MoS_2 PL is slightly broadened but with the peak energy not shifted. At a first glance, the absorption spectrum of the hybrid sample appears to be a superposition of the absorption of the individual components. A closer inspection of the spectrum reveals, however, that the absorption in the region of the low-energy feature of the Q-band is enhanced. This becomes clearer by taking the difference

of the absorption spectrum of the hybrid structure and the bare MoS_2 layer (see Fig. 3b and for comparison the H_2Pc absorption in Fig. 3a). A similar observation has previously been reported at MoS_2/H_2Pc and other MoS_2/metal-Pc interfaces and assigned to a charge transfer absorption involving a transition from the Pc's HOMO to the MoS_2 conduction band.[16,30] However, according to our PES experiments, the energy gap of this transition is 1.2 eV only, i.e. the charge transfer absorption should set in at much lower energy. This is in agreement with recent two photon photoemission spectroscopy on $ZnPc/MoS_2$ interfaces which reveal a relaxed charge transfer state with an energy of ca. 1.2 eV.[17] Furthermore, charge transfer transitions across hybrid interfaces have typically much lower oscillator strengths than the allowed optical transitions in the constituent materials.[31] H_2Pc molecules can crystallize in two principle phases, the so called α- and β-phase.[27,28] The phases possess slightly different absorption spectra. In particular, the low energy feature of the Q-band gains oscillator strength and slightly red-shifts in the β-phase and thus bears resemblance to the difference spectrum in Fig. 3b. It therefore seems more natural to explain the change in the absorption spectrum with a different packing of the H_2Pc molecules on SiO_2 and MoS_2 rather than to invoke the absorption of a hybrid charge transfer state.

Exciton dissociation at the MoS_2/H_2Pc interface should manifest itself in a shortening of the PL decay time since an additional decay channel for the excitons is generated. The PL decay in the present MoS_2 ML is comparable to the instrument response function (IRF) of the time-correlated single photon counting set-up (see Fig. 3c). Therefore, only the dynamics of H_2Pc excitons can be probed. Comparing the PL transients of H_2Pc in the hybrid structure and the reference sample, a clear shortening of the decay time from $\tau_{\mathrm{ref}} = 217$ ps (on SiO_2) to $\tau_{\mathrm{hyb}} \leq 34$ ps (on MoS_2) is observed (see Fig. 3c). Since the PL decay of the hybrid sample is close to the IRF, the derived value for τ_{hyb} has to be regarded as an upper bound. The effective efficiency of the exciton dissociation amounts thus to $\eta = 1 - \tau_{\mathrm{hyb}}/\tau_{\mathrm{ref}} \geq 0.85$ with an effective time constant of the exciton quenching of ≤ 50 ps. These effective values do not represent the electron transfer from the H_2Pc LUMO to the MoS_2 conduction band

only but include also the exciton diffusion to the hybrid interface. According to pump-probe measurements, the electron transfer can be as fast as < 320 fs.[16]

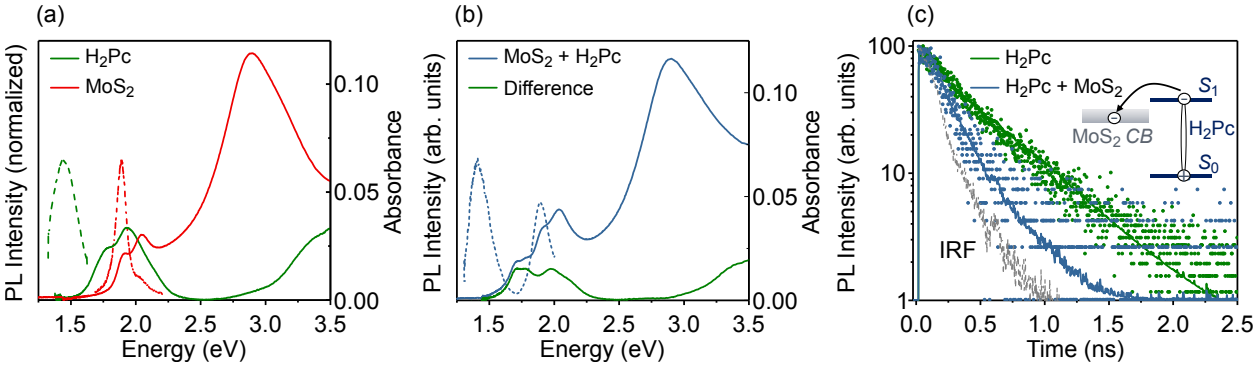

Figure 3: (a) Absorbance (solid lines) and PL (dashed lines) spectra of reference samples of a 3-nm thick H_2Pc film (green) and of a MoS_2 ML (red) on SiO_2 substrates. The PL spectra were obtained exciting the samples at 1.95 eV and 2.21 eV for H_2Pc and MoS_2, respectively. (b) PL (dashed blue line) excited at 2.21 eV and the corresponding absorption spectrum (solid blue line) of the MoS_2/H_2Pc hybrid structure on SiO_2. The H_2Pc layer thickness is $d_{H_2Pc} = 1.0$ nm. The green line represents the difference of the absorption spectra of the hybrid structure and the MoS_2 sample before the deposition of H_2Pc. (c) PL transients of H_2Pc in a reference sample on SiO_2 with a layer thickness of $d_{H_2Pc} = 1.0$ nm (green dots) and in the MoS_2/H_2Pc hybrid structure (blue dots). The excitation energy is 1.95 eV. The instrument response function (IRF) is shown as well (gray). The solid lines are fits to the data by convoluting exponential transients $N(t)$ with two components with the IRF according to $I(t) = \int_0^t IRF(t')N(t-t')dt'$. The lifetimes given in the text are time averages over these decay curves $\tau = \int t \cdot N(t)dt / \int N(t)dt$. The inset depicts the charge transfer from H_2Pc to the MoS_2 conduction band after photoexcitation of the sample.

For the generation of free charge carriers, exciton dissociation and charge transfer across the hybrid interface is only the first step. As an intermediate state, coulombically bound electron-hole pairs are likely to be formed. These so-called charge transfer excitons have been observed at various inorganic/organic interfaces.[31,32] More recently, indications for their occurrence also at an organic/TMDC interface have been found.[33] Only when the charge transfer excitons dissociate, free charge carriers are formed and a photoconductive response is generated. To probe the efficiency of this process, hybrid MoS_2/H_2Pc as well as reference H_2Pc- and MoS_2-only photodetectors were prepared. The design of the hybrid device is depicted in Fig. 4a. The hybrid and reference devices were prepared on SiO_2 substrates coated with a benzocylobutene (BCB)-based polymer layer. This layer was introduced to avoid the

formation of charged trap states which are commonly observed at MoS_2/SiO_2 interfaces and manifest themselves in a persisting photocurrent lasting for up to hours.[34–39] These trap states have been shown to override the photoresponse stemming from the TMDC/organic interface.[15] Since the dielectric constants for SiO_2 (3.7-3.9) and the BCB polymer (ca. 2.5-2.6)[40] are similar, the energy level alignment at the hybrid interface presented in Fig. 2 will be valid also for the devices. Photocurrent action spectra were recorded under external bias of the structure employing a modulation technique which guarantees that any residual contribution of persistent photoconductivity is removed from the spectra. The photoresponse spectra of the H_2Pc/MoS_2 hybrid and the MoS_2 reference photodetectors are shown in Fig. 4b. Whereas the photoresponse of the sole MoS_2 directly follows the absorption spectrum of MoS_2, additional features are clearly visible in the hybrid MoS_2/H_2Pc device. Their origin becomes evident when taking the difference $\Delta R = R_{\mathrm{hyb}} - R_{\mathrm{ref}}$ of the photoresponse spectra of the hybrid (R_{hyb}) and reference (R_{ref}) MoS_2-only device. The difference spectrum follows nicely the absorption spectrum of H_2Pc on MoS_2 (see for comparison Fig. 3b) with the contributions of the Q- and Soret bands clearly visible. The features can thus be assigned to a photoconductivity contribution arising due to absorption in the H_2Pc layer. Since the H_2Pc is a photoconductor by itself, the contribution could be due to the formation of a second photoconducting channel through the H_2Pc layer of the device. However, no photoconductivity signal could be detected in the H_2Pc-only device on a BCB covered SiO_2 substrate. The reason for this negative result becomes apparent when inspecting the H_2Pc film morphology on MoS_2 in the AFM image in Fig. 4c (on BCB, see Supporting Information). The H_2Pc film is discontinuous, consisting of three-dimensional islands with an average height of 5 nm. In such a film only few conductive paths can form so that the photocurrent signal falls below the detection limit. Most likely, the observed film morphology is a result of dewetting of the H_2Pc layer. Such dewetting of initially two-dimensional films is commonly observed in very thin molecular films on various insulator substrates (including MoS_2), in particular after air exposure.[41,42] For the purpose of the present study focusing on photocarrier generation by

charge transfer interactions at the hybrid interface, the three-dimensional film morphology of H_2Pc is beneficial, since the photoconduction within the organic layer has not to be accounted for. Therefore, no measures were taken to achieve homogeneous H_2Pc layers. The excitation density in the spectral range of the H_2Pc absorption is < 0.1 mW/cm^2 which corresponds to a very low exciton density of $< 5{\cdot}10^3$ excitons/cm^2 generated in the organic layer. While after dissociation, the electrons contribute to the photoconductivity in MoS_2, the holes are trapped in the molecular islands. The effect of the trapped holes on the potential profile across the H_2Pc/MoS_2 interface is, however, negligible due to their low density. For practical device applications, continuous two-dimensional H_2Pc layers are nevertheless desirable. In this way, also the H_2Pc layer could contribute to the photoconductivity of the device. Furthermore, the absorption of the device could be enhanced since the nominal organic layer thickness could be increased to match the exciton diffusion length in H_2Pc. The reported values in the literature range from 6.5 nm to 12 nm.[43]

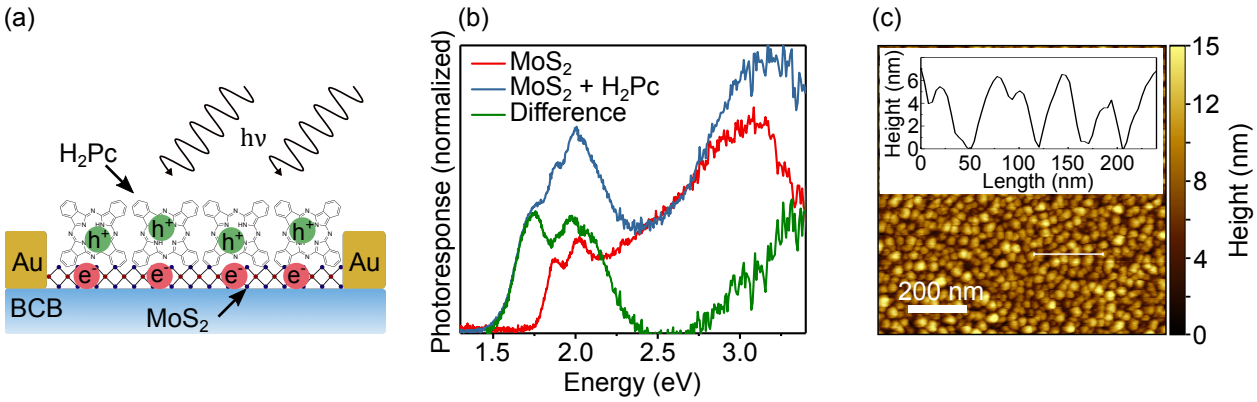

Figure 4: (a) Schematic design of the hybrid H_2Pc/MoS_2 photodetecting device. The H_2Pc layer thickness is $d_{H_2Pc} = 3.0$ nm. (b) Photoresponse of the hybrid (blue) and the reference MoS_2-only (red) device. The spectra were normalized at the spectral position where H_2Pc does not absorb, i.e. between 2.5-2.55 eV. Difference of the spectra of the hybrid (R_{hyb}) and reference (R_{ref}) device $\Delta R = R_{hyb} - R_{ref}$ (green). (c) AFM image of the morphology of a nominally 3-nm-thick H_2Pc film on MoS_2. The actual coverage is 0.85. The height scan was taken along the thin white line.

The observed excited state charge transfer increases the concentration of carriers n directly photogenerated in MoS_2 and with that its photoconductivity $\sigma = en\mu$ with μ being the mobility of the carriers. The contribution of the dissociated H_2Pc excitons to the enhance-

ment of the photoconductivity can be estimated from the photoresponse spectra of the hybrid and reference device normalized at a spectral position where H_2Pc does not absorb (see Fig. 4c). The normalization guarantees that the contributions of hole and/or exciton transfer from MoS_2 to H_2Pc are removed. At low excitation densities used in the present experiments, the ratio of indirectly Δn (via absorption in H_2Pc and subsequent electron transfer) to the directly n (via absorption in MoS_2) produced carriers is $\Delta n/n = \eta_i \alpha_{H_2Pc}/(\eta_d \alpha_{MoS_2})$. α_{MoS_2} and α_{H_2Pc} are the absorption coefficients of the respective layers and η_d (η_i) the quantum yields of the photocarrier generation via the direct (indirect) process. Under the assumption that the carrier mobility in MoS_2 does not change upon deposition of the molecules, which is reasonable since no signs of ground state electronic interactions were detected, $\Delta n/n = \Delta\sigma/\sigma$ holds. Comparing the photoresponse spectra of the reference and hybrid device in the spectral region of the lowest Q-band transition of H_2Pc and the A excitonic transition in MoS_2, the ratio $\Delta n/n$ is roughly one. The absorption spectra in Fig. 3a also yield $\alpha_{H_2Pc}/\alpha_{MoS_2} \approx 1$ (see Fig. 3a), which implies that the quantum yields of the photocarrier generation of the direct and indirect process are comparable in the present device configuration.

Conclusions

The presented experimental data demonstrate that the photoresponse of ML-MoS_2 in hybrid MoS_2/H_2Pc photodetectors is strongly enhanced and furthermore without loss in sensitivity extended to spectral regions were the TMDC is transparent. The observation is explained by the staggered type II energy level alignment at the hybrid interface facilitating efficient exciton dissociation and excited state charge transfer with the holes residing in the H_2Pc HOMO and the electrons in the MoS_2 conduction band. In hybrid photodetectors, these transferred charges increase the concentration of carriers in MoS_2 and with that its photoconductivity. In the present configuration, the quantum yields of the photocarrier generation by direct absorption in MoS_2 and by absorption in H_2Pc followed by excited state charge transfer are

comparable ($\eta_d \approx \eta_i$). This result can be further improved. In the studied devices, the H_2Pc film is not homogeneous but consists of three-dimensional islands. However, only the molecules in close proximity can engage in fast charge transfer.[44] It is furthermore well-known that the orientation of the molecules with respect to the interface and the crystallinity of the molecular film have strong impact on the excited state charge transfer.[45] It can therefore be expected that optimization of the growth of H_2Pc on MoS_2 enables even $\eta_i > \eta_d$ for this material combination. This can be achieved by a proper adjustment of the deposition rate and the substrate temperature, since these parameters determine the nucleation density in a diffusion-mediated growth process, and thus, the smoothness and crystallinity of the organic layer. In the present photodetector the spectral sensitivity range is extended by 250 meV towards smaller photon energies. By choice of molecules with smaller optical gap than H_2Pc, the range can easily be further expanded and true functionality added to the TMDC.

Supporting Information Available

XPS Mo 3d and S 2p core level spectra of the MoS_2/H_2Pc interface, IPES raw data and a comparison of AFM images of H_2Pc on BCB and MoS_2 are available in the supporting information.

Acknowledgement

This work was funded by the Deutsche Forschungsgemeinschaft (DFG, German Research Foundation)-Project No. 182087777-SFB 951.

References

(1) Mak, K. F.; Lee, C.; Hone, J.; Shan, J.; Heinz, T. F. Atomically Thin MoS_2: A New Direct-Gap Semiconductor. *Phys. Rev. Lett.* **2010**, *105*, 136805.

(2) Chernikov, A.; Berkelbach, T. C.; Hill, H. M.; Rigosi, A.; Li, Y.; Aslan, O. B.; Reichman, D. R.; Hybertsen, M. S.; Heinz, T. F. Exciton Binding Energy and Nonhydrogenic Rydberg Series in Monolayer WS_2. *Phys. Rev. Lett.* **2014**, *113*, 076802.

(3) Schmidt, H.; Giustiniano, F.; Eda, G. Electronic Transport Properties of Transition Metal Dichalcogenide Field-Effect Devices: Surface and Interface Effects. *Chem. Soc. Rev.* **2015**, *44*, 7715–7736.

(4) Radisavljevic, B.; Radenovic, A.; Brivio, J.; Giacometti, V.; Kis, A. Single-Layer MoS_2 Transistors. *Nat. Nanotechnol.* **2011**, *6*, 147–150.

(5) Gu, J.; Liu, X.; Lin, E.-c.; Lee, Y.-H.; Forrest, S. R.; Menon, V. M. Dipole-Aligned Energy Transfer Between Excitons in Two-Dimensional Transition Metal Dichalcogenide and Organic Semiconductor. *ACS Photonics* **2017**, *5*, 100–104.

(6) Cheng, C.-H.; Li, Z.; Hambarde, A.; Deotare, P. B. Efficient Energy Transfer Across Organic-2D Inorganic Heterointerfaces. *ACS Appl. Mater. Interfaces* **2018**, *10*, 39336–39342.

(7) Liu, X.; Gu, J.; Ding, K.; Fan, D.; Hu, X.; Tseng, Y.-W.; Lee, Y.-H.; Menon, V.; Forrest, S. R. Photoresponse of an Organic Semiconductor/Two-Dimensional Transition Metal Dichalcogenide Heterojunction. *Nano Lett.* **2017**, *17*, 3176–3181.

(8) Zhong, C.; Sangwan, V. K.; Wang, C.; Bergeron, H.; Hersam, M. C.; Weiss, E. A. Mechanisms of Ultrafast Charge Separation in a PTB7/Monolayer MoS_2 van der Waals Heterojunction. *J. Phys. Chem. Lett.* **2018**, *9*, 2484–2491.

(9) Bettis Homan, S.; Sangwan, V. K.; Balla, I.; Bergeron, H.; Weiss, E. A.; Hersam, M. C. Ultrafast Exciton Dissociation and Long-Lived Charge Separation in a Photovoltaic Pentacene-MoS_2 van der Waals Heterojunction. *Nano Lett.* **2017**, *17*, 164–169.

(10) Park, J. H.; Sanne, A.; Guo, Y.; Amani, M.; Zhang, K.; Movva, H. C. P.; Robinson, J. A.; Javey, A.; Robertson, J.; Banerjee, S. K. et al. Defect Passivation of Transition Metal Dichalcogenides via a Charge Transfer van der Waals Interface. *Sci. Adv.* **2017**, *3*, e1701661.

(11) Kafle, T. R.; Kattel, B.; Lane, S. D.; Wang, T.; Zhao, H.; Chan, W.-L. Charge Transfer Exciton and Spin Flipping at Organic-Transition-Metal Dichalcogenide Interfaces. *ACS Nano* **2017**, *11*, 10184–10192.

(12) Choi, J.; Zhang, H.; Choi, J. H. Modulating Optoelectronic Properties of Two-Dimensional Transition Metal Dichalcogenide Semiconductors by Photoinduced Charge Transfer. *ACS Nano* **2016**, *10*, 1671–1680.

(13) Pak, J.; Jang, J.; Cho, K.; Kim, T.-Y.; Kim, J.-K.; Song, Y.; Hong, W.-K.; Min, M.; Lee, H.; Lee, T. Enhancement of Photodetection Characteristics of MoS_2 Field Effect Transistors Using Surface Treatment with Copper Phthalocyanine. *Nanoscale* **2015**, *7*, 18780–18788.

(14) Nguyen, E. P.; Carey, B. J.; Harrison, C. J.; Atkin, P.; Berean, K. J.; Della Gaspera, E.; Ou, J. Z.; Kaner, R. B.; Kalantar-Zadeh, K.; Daeneke, T. Excitation Dependent Bidirectional Electron Transfer in Phthalocyanine-Functionalised MoS_2 Nanosheets. *Nanoscale* **2016**, *8*, 16276–16283.

(15) Huang, Y.; Zhuge, F.; Hou, J.; Lv, L.; Luo, P.; Zhou, N.; Gan, L.; Zhai, T. Van der Waals Coupled Organic Molecules with Monolayer MoS2 for Fast Response Photodetectors with Gate-Tunable Responsivity. *ACS Nano* **2018**, *12*, 4062–4073.

(16) Padgaonkar, S.; Amsterdam, S. H.; Bergeron, H.; Su, K.; Marks, T. J.; Hersam, M. C.; Weiss, E. A. Molecular-Orientation-Dependent Interfacial Charge Transfer in Phthalocyanine/MoS_2 Mixed-Dimensional Heterojunctions. *J. Phys. Chem. C* **2019**, *123*, 13337–13343.

(17) Kafle, T. R.; Kattel, B.; Yao, P.; Zereshki, P.; Zhao, H.; Chan, W.-L. Effect of the Interfacial Energy Landscape on Photoinduced Charge Generation at the ZnPc/MoS_2 Interface. *J. Am. Chem. Soc.* **2019**, *141*, 11328–11336.

(18) Park, S.; Mutz, N.; Schultz, T.; Blumstengel, S.; Han, A.; Aljarb, A.; Li, L.-J.; List-Kratochvil, E. J. W.; Amsalem, P.; Koch, N. Direct Determination of Monolayer MoS_2 and WSe_2 Exciton Binding Energies on Insulating and Metallic Substrates. *2D Mater.* **2018**, *5*, 025003.

(19) Mutz, N.; Meisel, T.; Kirmse, H.; Park, S.; Severin, N.; Rabe, J. P.; List-Kratochvil, E.; Koch, N.; Koch, C. T.; Blumstengel, S. et al. Pulsed Thermal Deposition of Binary and Ternary Transition Metal Dichalcogenide Monolayers and Heterostructures. *Appl. Phys. Lett.* **2019**, *114*, 162101.

(20) Gurarslan, A.; Yu, Y.; Su, L.; Yu, Y.; Suarez, F.; Yao, S.; Zhu, Y.; Ozturk, M.; Zhang, Y.; Cao, L. Surface-Energy-Assisted Perfect Transfer of Centimeter-Scale Monolayer and Few-Layer MoS_2 Films onto Arbitrary Substrates. *ACS Nano* **2014**, *8*, 11522–11528.

(21) Raja, A.; Chaves, A.; Yu, J.; Arefe, G.; Hill, H. M.; Rigosi, A. F.; Berkelbach, T. C.; Nagler, P.; Schüller, C.; Korn, T. et al. Coulomb Engineering of the Bandgap and Excitons in Two-Dimensional Materials. *Nat. Commun.* **2017**, *8*, 15251.

(22) Park, S.; Schultz, T.; Han, A.; Aljarb, A.; Xu, X.; Beyer, P.; Opitz, A.; Ovsyannikov, R.; Li, L.-J.; Meissner, M. et al. Electronic Band Dispersion Determination in Azimuthally Disordered Transition-Metal Dichalcogenide Monolayers. *Commun. Phys.* **2019**, *2*, 288.

(23) Park, S.; Schultz, T.; Xu, X.; Wegner, B.; Aljarb, A.; Han, A.; Li, L.-J.; Tung, V. C.; Amsalem, P.; Koch, N. Demonstration of the Key Substrate-Dependent Charge Transfer Mechanisms Between Monolayer MoS2 and Molecular Dopants. *Commun. Phys.* **2019**, *2*, 699.

(24) Keyshar, K.; Berg, M.; Zhang, X.; Vajtai, R.; Gupta, G.; Chan, C. K.; Beechem, T. E.; Ajayan, P. M.; Mohite, A. D.; Ohta, T. Experimental Determination of the Ionization Energies of MoSe2, WS2, and MoS2 on SiO2 Using Photoemission Electron Microscopy. *ACS Nano* **2017**, *11*, 8223–8230.

(25) Zahn, D. R.; Gavrila, G. N.; Gorgoi, M. The Transport Gap of Organic Semiconductors Studied Using the Combination of Direct and Inverse Photoemission. *Chem. Phys.* **2006**, *325*, 99–112.

(26) MacKeown, N. B. *Phthalocyanine Materials: Synthesis, Structure and Function*; Chemistry of Solid State Materials; Cambridge Univ. Press: Cambridge, 1998; Vol. 6.

(27) Heutz, S.; Bayliss, S. M.; Middleton, R. L.; Rumbles, G.; Jones, T. S. Polymorphism in Phthalocyanine Thin Films: Mechanism of the $\alpha \rightarrow \beta$ Transition. *J. Phys. Chem. B* **2000**, *104*, 7124–7129.

(28) Yim, S.; Heutz, S.; Jones, T. S. Model for the $\alpha \rightarrow \beta 1$ Phase Transition in Phthalocyanine Thin Films. *J. Appl. Phys.* **2002**, *91*, 3632–3636.

(29) Yoshida, H.; Tokura, Y.; Koda, T. Charge-Transfer Excitation Bands in Electro-Absorption Spectra of Metal (Co, Ni, Cu, Zn)-Phthalocyanine Films. *Chem. Phys.* **1986**, *109*, 375–382.

(30) Amsterdam, S. H.; Stanev, T. K.; Zhou, Q.; Lou, A. J.-T.; Bergeron, H.; Darancet, P.; Hersam, M. C.; Stern, N. P.; Marks, T. J. Electronic Coupling in Metallophthalocyanine-Transition Metal Dichalcogenide Mixed-Dimensional Heterojunctions. *ACS Nano* **2019**, *13*, 4183–4190.

(31) Piersimoni, F.; Schlesinger, R.; Benduhn, J.; Spoltore, D.; Reiter, S.; Lange, I.; Koch, N.; Vandewal, K.; Neher, D. Charge Transfer Absorption and Emission at ZnO/Organic Interfaces. *J. Phys. Chem. Lett.* **2015**, *6*, 500–504.

(32) Eyer, M.; Frisch, J.; Sadofev, S.; Koch, N.; List-Kratochvil, E. J. W.; Blumstengel, S. Role of Hybrid Charge Transfer States in the Charge Generation at ZnMgO/P3HT Heterojunctions. *J. Phys. Chem. C* **2017**, *121*, 21955–21961.

(33) Zhu, T.; Yuan, L.; Zhao, Y.; Zhou, M.; Wan, Y.; Mei, J.; Huang, L. Highly Mobile Charge-Transfer Excitons in Two-Dimensional WS_2/Tetracene Heterostructures. *Sci. Adv.* **2018**, *4*, eaao3104.

(34) Di Bartolomeo, A.; Genovese, L.; Foller, T.; Giubileo, F.; Luongo, G.; Croin, L.; Liang, S.-J.; Ang, L. K.; Schleberger, M. Electrical Transport and Persistent Photoconductivity in Monolayer MoS_2 Phototransistors. *Nanotechnology* **2017**, *28*, 214002.

(35) Zhang, W.; Huang, J.-K.; Chen, C.-H.; Chang, Y.-H.; Cheng, Y.-J.; Li, L.-J. High-Gain Phototransistors Based on a CVD MoS_2 Monolayer. *Adv. Mater.* **2013**, *25*, 3456–3461.

(36) Lopez-Sanchez, O.; Lembke, D.; Kayci, M.; Radenovic, A.; Kis, A. Ultrasensitive Photodetectors Based on Monolayer MoS_2. *Nat. Nanotechnol.* **2013**, *8*, 497–501.

(37) Lee, Y.; Yang, J.; Lee, D.; Kim, Y.-H.; Park, J.-H.; Kim, H.; Cho, J. H. Trap-Induced Photoresponse of Solution-Synthesized MoS_2. *Nanoscale* **2016**, *8*, 9193–9200.

(38) Kufer, D.; Konstantatos, G. Highly Sensitive, Encapsulated MoS_2 Photodetector with Gate Controllable Gain and Speed. *Nano Lett.* **2015**, *15*, 7307–7313.

(39) Furchi, M. M.; Polyushkin, D. K.; Pospischil, A.; Mueller, T. Mechanisms of Photoconductivity in Atomically Thin MoS_2. *Nano Lett.* **2014**, *14*, 6165–6170.

(40) Modafe, A.; Ghalichechian, N.; Kleber, B.; Ghodssi, R. Electrical Characterization of Benzocyclobutene Polymers for Electric Micromachines. *IEEE Trans. Device Mater. Reliab.* **2004**, *4*, 495–508.

(41) Burke, S. A.; Topple, J. M.; Grütter, P. Molecular Dewetting on Insulators. *Journal Phys.: Condens. Matter* **2009**, *21*, 423101.

(42) Zhang, L.; Yang, Y.; Huang, H.; Lyu, L.; Zhang, H.; Cao, N.; Xie, H.; Gao, X.; Niu, D.; Gao, Y. Thickness-Dependent Air-Exposure-Induced Phase Transition of CuPc Ultrathin Films to Well-Ordered One-Dimensional Nanocrystals on Layered Substrates. *J. Phys. Chem. C* **2015**, *119*, 4217–4223.

(43) Mikhnenko, O. V.; Blom, P. W. M.; Nguyen, T.-Q. Exciton Diffusion in Organic Semiconductors. *Energy Environ. Sci.* **2015**, *8*, 1867–1888.

(44) Dutton, G. J.; Robey, S. W. Distance Dependence of Exciton Dissociation at a Phthalocyanine-C60 Interface. *J. Phys. Chem. C* **2013**, *117*, 25414–25423.

(45) Yang, B.; Yi, Y.; Zhang, C.-R.; Aziz, S. G.; Coropceanu, V.; Brédas, J.-L. Impact of Electron Delocalization on the Nature of the Charge-Transfer States in Model Pentacene/C60 Interfaces: A Density Functional Theory Study. *J. Phys. Chem. C* **2014**, *118*, 27648–27656.

TOC Graphic

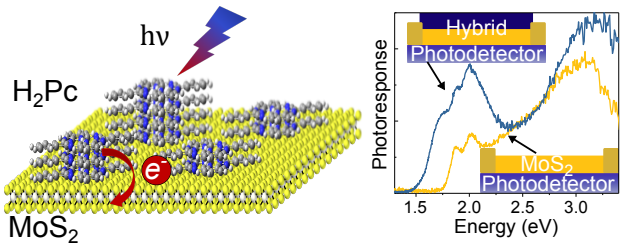
hν
H_2Pc
e⁻
MoS_2
Hybrid
Photodetector
MoS_2
Photodetector
Photoresponse
1.5
2.0
2.5
3.0
Energy (eV)